Analysis of Orientation Effects of Crop Vegetation Volumes by Means of SAR Tomography at Different Frequencies

Hannah Joerg[1,2], Matteo Pardini[1], Konstantinos P. Papathanassiou[1], Irena Hajnsek[1,2]
[1] German Aerospace Center - Microwaves and Radar Institute, Wessling, Germany
[2] ETH Zurich - Institute of Environmental Engineering, Zurich, Switzerland
Email: hannah.joerg@dlr.de

Abstract

Synthetic aperture radar (SAR) tomography is a powerful approach to investigate the relationship between 3-D radar backscattering and physical structure of agricultural vegetation, which is not fully understood yet. In this paper, the focus is set on the characterization of polarimetric scattering and propagation effects within the vegetation layer as a function of species, time and frequency. This is done by separating the ground and volume scattering contributions applying a coherent layer cancellation to the multi-baseline (MB) multi-polarimetric SAR data set. The analysis of the herewith retrieved powers of the individual components supported by ground-measurements help to understand better the effect of physical change on the electromagnetic scattering behaviour. To assess the presence of orientation effects, a distance measure is applied to the volume-only coherences to decide if they fit the random volume or the general oriented volume model. The experimental analysis is performed on multi-frequency data acquired by the DLR airborne sensor F-SAR.

1 Introduction

For the retrieval of bio- and geophysical parameters from polarimetric and interferometric SAR images of agricultural vegetation, generally a non-uniform orientation distribution of the volume particles causing a differential extinction between the polarizations is assumed [1, 2]. Such orientation effects are difficult to be characterized since they depend on species, development stage and wavelength. For instance, depending on the scattering particles causing the orientation effects, higher or lower frequencies might suffer more or less differential extinction. A quantitative analysis of differential extinction as a function of species, time and frequency would provide important information for the electromagnetic modelling of agricultural crop volumes.

In order to investigate the presence of differential extinction effects, the variation of the interferometric coherences with polarization can be analyzed. Tomographic SAR methodologies provide a possibility to do this by estimating the 3-D scattering distribution from the variation of phase and amplitude across the different tracks [3]. For vegetated agricultural fields, it is assumed that the scattering can be decomposed into ground and volume contributions. In order to assess the presence of orientation effects in the latter, a first step is the separation of ground and volume, here performed by a coherent layer cancellation [4]. In the case of a random volume the MB volume-only coherences and the related variation of the reflectivity profile along height do not vary with polarization, while they are polarization-dependent in the presence of differential propagation effects (i.e. extinction). Therefore, in this paper, the degree of polarization dependency of the vertical structure is quantified by evaluating the difference of the MB volume-only coherences from the ones obtained assuming a random volume model. Together with the variation of the ground and volume powers across the different polarizations and supported by the ground measurements, this analysis is used to get a better understanding of the physical scattering mechanisms inside the vegetation volumes depending on species, development stage and frequency. Finally, the effect of limited vertical resolution on the separation performance as well as the measure for the strucutral differences between the polarizations is evaluated.

The experimental analysis is performed on several fully polarimetric MB SAR data sets at X-, C- and L-band acquired by the DLR airborne sensor F-SAR. The data sets cover different dates in the phenological cycle. Insitu measurements of soil and vegetation parameters were collected in parallel to the acquisitions.

2 Volume Characterization

Orientation effects inside a scattering medium can be detected by testing the validity of a random volume over ground model. Such a test can be realized by investigating the linearity of the polarimetric interferometric single-baseline coherences [5].

Here we propose a different approach, which consists in investigating the MB multi-polarimetric coherences jointly. First of all, volume-only coherences have to be separated from the ground ones. If the more general volume orientation hypothethis is retained, in contrast to the case of a random volume [6], no decomposition for the polarimetric MB coherences exists. The solution proposed here exploits the location of the scattering contributions in height, assuming that the ground topography z_G is provided (e.g. from a digital terrain model acquired before the gowing period or produced by tomographic techniques [7]). No further models are needed to describe the

profile.

2.1 Coherent Layer Cancellation

For each polarization channel (HH, VV and HV) a MB data vector consisting of K images is available. For the processing, a multi-look cell with N independent looks is used and the K-dimensional MB data vector in the n-th look is represented by $\mathbf{y}(n)$.
The scattering mechanisms are separated based on the a priori knowledge of the location of the ground scattering centered at z_G and the assumption that the volume scattering is located certainly above the ground until 4 m height (from the ground measurements, no crop height has a full height higher than 3.5 m). With that, a filter is designed in order to cancel as much as possible the power components in a "stop band" around the ground location, $z \in [z_G - 0.2\,\text{m}, z_G + 0.2\,\text{m}]$, and to leave unaltered the volume scattering components in a "pass band", with $z \in [z_G + 0.3\,\text{m}, z_G + 4\,\text{m}]$ [4]. The result of this design is a filter in the form of a matrix $\mathbf{H}$. The volume only data vector $\mathbf{y}_V(n)$ is obtained as:

$$\mathbf{y}_V(n) = \mathbf{H}\mathbf{y}(n), \quad \forall n \in [0, N]. \tag{1}$$

The response of the designed filter $\mathbf{H}$ (with $z_G = 0\,\text{m}$) applied to a set of steering vectors $\mathbf{a}(z)$, with $z \in [-1\,\text{m}, 4\,\text{m}]$, is shown in Fig. 1. The cancellation amplitude in the ground phase center is below -20 dB, while the response in the pass band is retained as required (0 dB). This approach has the advantage that the coherent structure of the data is preserved for the filtered data allowing to perform any polarimetric and interferometric processing [4].

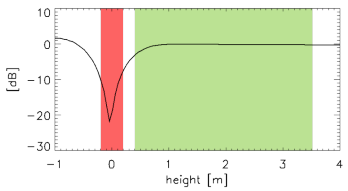

Figure 1: Response of the matrix filter $\mathbf{H}$ to an array of steering vectors $\mathbf{a}(z)$, with $z \in [-1\,\text{m}, 4\,\text{m}]$ (red: stop band, green: pass band).

It is assumed that the total MB covariance matrix is the sum of two components: a ground component with power p_G and a vertical structure which is compact in height compared to the vertical resolution; and a volume component with power p_V and structure retrieved from (1). The maximum likelihood estimates for p_G and p_V can then be calculated by minimizing the difference between the MB data covariance matrix and the sum of the above described ground and volume component in a least squares sense [8]. In cases where the plant height is in the order of the vertical resolution and the two components are within the same resolution cell, the seperation becomes more challenging. Simulations showed that this affects mainly the estimation of p_G for low ground-to-volume ratios. While the root-mean-square error for p_V is always below 10% it increases for p_G from 10% (2 height resolution units) up to 30% for a ground-to-volume ratio of 5 dB for only one height resolution unit.

2.2 Orientation Effects

The polarimetric MB volume coherency matrix is formed from the volume only data vectors retrieved for each polarization channel as in equation (1): $\mathbf{R}_V = \mathbf{y}_V^{pol}\mathbf{y}_V^{pol\,H}$, where $\mathbf{y}_V^{pol} = \left[\mathbf{y}_V^{HH}\mathbf{y}_V^{HV}\mathbf{y}_V^{VV}\right]^T$. In the case of no orientation effects, i.e. if the random volume hypothesis holds, the MB volume coherences $\mathbf{R}_V^{(RV)}$ can be obtained in closed form by fitting the Kronecker product model in [6] limited to one scattering mechanism to the MB volume coherences $\mathbf{R}_V$. Then, the significance of orientation effects inside the vegetation volume can be assessed by the difference between the volume coherences for the random volume hypothesis, $\mathbf{R}_V^{(RV)}$, and the ones for the general, oriented volume hypothesis, $\mathbf{R}_V$. Note that, here, the MB volume coherences and not the covariances are used in order to ensure sensitivity to differences in structure and not in powers. The distance is quantified using the normalized Frobenius norm:

$$\Delta = \frac{\|\mathbf{R}_V^{(RV)} - \mathbf{R}_V\|_F}{\|\mathbf{R}_V\|_F}. \tag{2}$$

Another possibility to test the randomness of the vegetation volume is to use a statistical test for the random volume hypothesis [9]. However, the retrieved volume coherences in $\mathbf{R}_V$ do not necessarily fulfill certain statistical requirements for the application of the proposed test. Therefore, the Frobenius norm is chosen here despite the averaging across all the elements of the difference between the coherency matrices can lead to low sensitivity in some cases.

3 Experimental Results

3.1 Test Site and Data Set

The experimental data set was acquired by the DLR airborne sensor F-SAR over an agricultural area near Wallerfing (in southern Germany) in 2014. From May to August, 8 fully polarimetric MB data sets at X- and C-band and 7 data sets at L-band were acquired. The amplitude image (on July 03) in Fig. 2 shows the part of the scene where the analysis is carried out. The landuse is indicated by the color of the field borders: yellow for corn, green for wheat and red for barley. The fields C1, C2, W and B are evaluated more in detail in the following. The table next to the patch lists the number of tracks acquired in each flight and the value of the maximum vertical wavenumber k_z for the different frequencies at an incidence angle of 30°. The resulting Rayleigh resolution in the middle of the patch is 0.5 m in X-band, 0.8 m in C-band, 1.4 m in L-band.

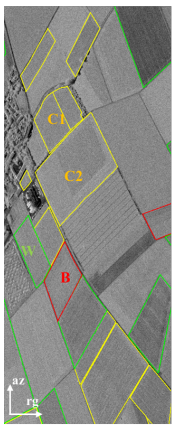

Acquisition settings			
flight	date	# tracks, max. kz (at 30° inc. angle)	
		X / C	L
02	May 15	3 12.5/7.8 m^{-1}	3 4.5 m^{-1}
03	May 22	9 12.5/7.8 m^{-1}	8 4.5 m^{-1}
06	June 4	9 12.5/7.8 m^{-1}	6 4.5 m^{-1}
07	June 12	9 12.5/7.8 m^{-1}	7 4.5 m^{-1}
09	June 18	8 12.5/7.8 m^{-1}	7 4.5 m^{-1}
11	July 3	9 12.5/7.8 m^{-1}	8 4.5 m^{-1}
13	July 24	9 12.5/7.8 m^{-1}	7 4.5 m^{-1}
15	Aug 24	5 12.5/7.8 m^{-1}	---

Figure 2: Left: HH amplitude image of the patch on July 03 at C-band with landuse. C1, C2, W and B indicate the fields of interest. Right: Table with acquisition settings.

The tomographic processing of the data was carried out using a multi-look cell of 7.5×7.5 m, corresponding to approximately 220 independent looks at X- and C-band and 100 independent looks at L-band. The topographic phase is assumed known from a Lidar DTM and it is compensated in the MB data.

In the following, the results on the corn fields are discussed first, since the height of the vegetation reaches more than three Rayleigh resolution units in the end of the phenological cycle. In this case, a tomographic inversion is less critical than for plant heights in the order of the vertical Rayleigh resolution, like in wheat and barley, which are discussed later.

3.2 Structural Analysis of Corn

3.2.1 C-band

Ground measurements corn fields C1 and C2				
flight	date	average plant height	average soil moisture	average vegetation water content
02	May 15	0.05m	23 vol%	----
03	May 22	0.1m	18 vol%	----
06	June 4	0.3m	18 vol%	----
07	June 12	0.5-0.7m	10 vol%	90%
09	June 18	0.7-1m	11 vol%	80%
11	July 3	1.5-1.9m	23 vol%	91%
13	July 24	3.1-3.5m	17 vol%	86%
15	Aug 4	3.1-3.4m	14 vol%	81%

Table 1: Ground measurements in corn fields C1 and C2 on the acquisition dates.

Table 1 provides mean values of the ground measurements (such as plant height, soil moisture and vegetation water content) collected in parallel to the acquisitions in the corn fields C1 and C2. The study period covers the whole growth period of the plants until ripening.

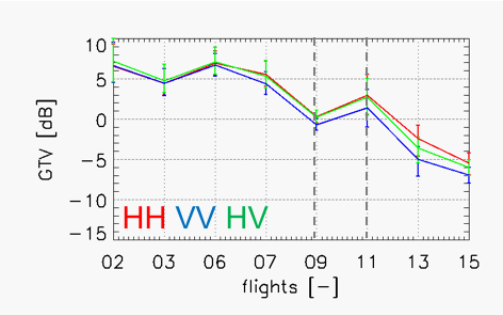

Figure 3: Variation of the ground-to-volume power ratio in C1 and C2 over the acquisition period.

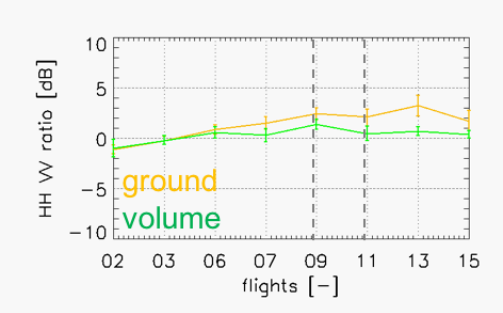

Figure 4: Variation of the co-polar power ratio in C1 and C2 over the acquisition period.

Fig. 3 shows the variation of the ground-to-volume power ratio over the acquisition period for the different polarizations. The co-polar ratio of the retrieved powers for the ground and the volume component for the different acquisition dates is presented in Fig. 4. The variation of the scattering behaviour can be divided in three parts (indicated by the grey dashed lines in Fig. 3 and 4). In the first time interval, the ground-to-volume power ratio is mainly decreasing which was found to be due to an increase in p_V related to the starting growth of the plants. Even though it is possible that the ground-to-volume ratio is overestimated for low plant heights below the vertical Rayleigh resolution the decreasing trend can be trusted since the ground component p_G is more affected by inacurrate estimation while the conclusions drawn here are based on the change in p_V. In the second interval, an increase of the ground-to-volume ratio is observed which is related to a change from dry to wet soil (11 vol% to 23 vol%) causing the ground power p_G to increase while p_V stays constant. During the third time period, the ground-to-volume ratio decreases again due to a decrease in p_G while p_V stays constant even though the plant growth continues until maximum height in flight 13 and 15. Additionally, the decrease in p_G is much bigger than expected for the soil moisture change from flight 11 to 13. The reason could be a change in vegetation structure. The radiometric height of the total power vertical profile given by the highest position in height where the 3-D total power is 3 dB lower than the maximum peak in relation to the measured plant heights (see Fig. 5) helps to understand this change.

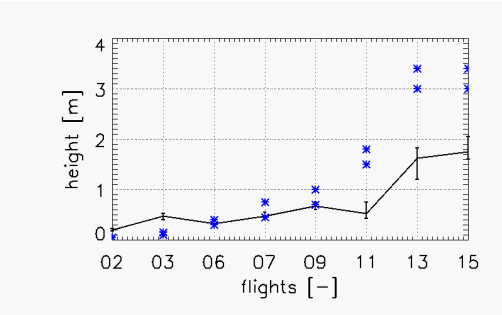

Figure 5: Variation of the radiometric height related to the upper and lower boundary of the measured heights (blue) over the acquisition period.

In the first two flights the radiometric height is above the measured values because the plants are lower than the vertical extension assumed for the ground. In flights 06-09 the radiometric height is very close to the measured plant heights in these dates. In the later flights, the measured plant height is 1.5 to 2 times higher than the radiometric height. This indicates that despite the ongoing growth of the plants, the upper part becomes electromagnetically more transparent. The plant development in these flights is already advanced. While in flight 11 the fruit is not yet present, the fruit development is in the "early milk" stage in flight 13 and the ripening starts in flight 15 where the "dough stage" is reached. In these later development stages the main scattering contribution seems to come from the middle part of the plant and at the same time extinction increases. Hence, less power comes from the ground and the volume contribution stays constant.

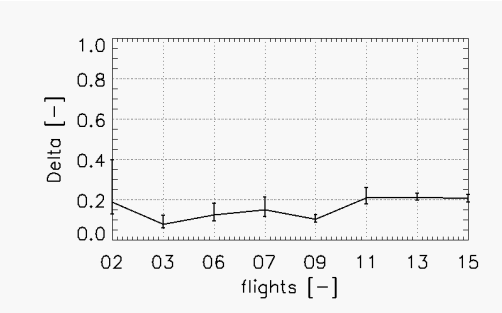

Figure 6: Variation of the normalized Frobenius distance Δ in C1 and C2 over the acquisition period.

The co-polar ratio of the volume component (Fig. 4) shows negligible deviation from zero for all the acquisition dates suggesting that the volume scattering and hence the structure in HH and VV are similar. The normalized Frobenius distance Δ depicted in Fig. 6 shows only small variations until flight 09 while Δ is always around 0.2 in flight 11-15. In flight 11 the plant height exceeds for the first time clearly the Rayleigh resolution which certainly contributes to the increase of Δ. Even though for flights 13 and 15 approximately 3 height resolution units are available, Δ does not increase further. When retrieving the ground and volume powers using the random volume MB coherences $\mathbf{R}_V^{(RV)}$ no significant difference was found compared to the non-model based volume assumption. This fact, together with the negligible variation of the co-polar power ratio of the volume, suggests that despite the higher values of Δ in flight 11-15 structural differences between the polarizations and therefore orientation are not significant.

This fact could also be related to the high number of looks leading to an averaging of possibly oriented structures, especially since the distance between the rows of the corn plants ranges from 70-85 cm. In order to understand this impact, Δ is calculated with a smaller multi-look cell of only 2.7×2.7 m corresponding to 30 independent looks.

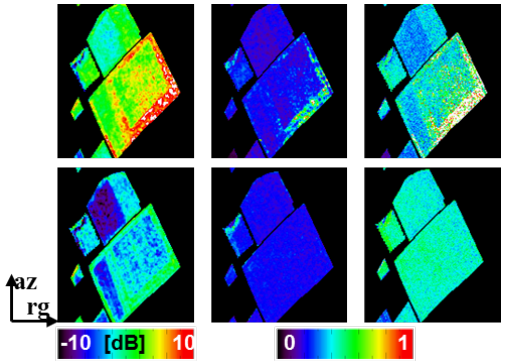

Figure 7: Left: ground-to-volume power ratio at HH; middle: Δ for 220 looks; right Δ for 30 looks in C1 and C2 for flight 11 (top) and 13 (bottom).

Fig. 7 shows the ground-to-volume ratio in HH for reference (left), Δ for the original number of looks (middle) and for the smaller multi-look cell (right) in flight 11 (top) and 13 (bottom). While the inverted powers do not change sensitively, Δ retrieved using less looks is higher and, particularly in flight 11, more diverse within the corn fields. In flight 11, it can be observed that Δ is higher in areas with higher ground-to-volume ratio. This can be explained with the row orientation and the row distance of the corn plants measured during the ground campaign. At the sides of field C2, the rows are rather directed towards the line of sight corresponding to the areas with highest ground-to-volume ratio. Further, the rows are closer in C2 at steeper incidence angle. In C1, the row distance is bigger at steeper incidence angle than in the area with lower ground-to-volume ratio at shallower incidence angle. Hence, a smaller row distance leads to a lower scattering contribution from the ground and respectively a higher p_V. In flight 11, even for a smaller number of looks the structural differences are also lower in the areas with the smaller gaps, since there the electromagnetic wave is not sensitive to the stalks in the lower part of the plant but attenuated due to scattering from particles in the middle part of the plants. In contrast, in flight 13 the structural differences, even though they are higher for less looks, are less diverse within the fields. This can be explained by the higher plants at this date and less sensitivity to the gaps between the rows (as already observed from the power ratio analysis above).

3.2.2 X- and L-band

Fig. 8 shows the ground-to-volume ratio at HH for flights 11 (top) and flight 13 (bottom) at X- (left), C- (middle) and L-band (right). When moving from C- to X-band the ground-to-volume ratio becomes lower in both fields. The decrease from flight 11 to flight 13 is also at X-band mainly due to a decrease in p_G but different to C-band p_V additionally increases. Besides, the co-polar ratios for ground and volume, as well as Δ, show a similar behaviour as in C-band.

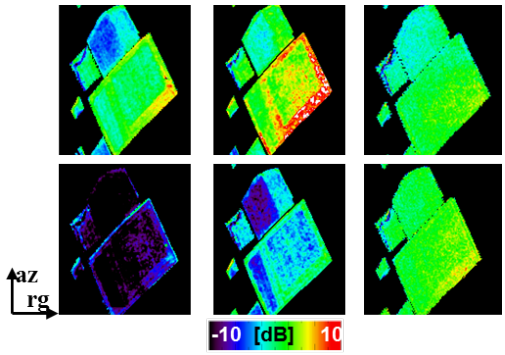

Figure 8: Ground-to-volume power ratio in C1 and C2 at HH at X-, C- and L-band (from left to right) for flight 11 (top) and 13 (bottom) .

At L-band the ground-to-volume ratio is now less diverse within the fields than at the higher frequencies. Unexpectedly, in flight 11 it is in some areas lower than at C-band. This might be explained by the almost six times longer wavelength resulting in less sensitivity to the gaps between the rows at L-band. In flight 13 instead the ground-to-volume ratio at L-band is higher compared to the higher frequencies. Besides, p_V is up to 4 dB higher in VV than in HH and also the VV volume phase center is up to 1 m higher than the one in HH in some areas while in the higher frequencies almost no differences between the polarizations are observed. Also Δ increases from flight 11 to 13 reaching a higher level than at X- or C-band. This indicates that the longer wavelength is more sensitive to the vertically oriented stalks resulting in a stronger polarization dependency at L-band in this later development stage.

3.3 Analysis of Wheat and Barley

For wheat and barley the plant height never exceeds 1 m, which is in the order of the vertical Rayleigh resolution. Since ground and volume component are within one resolution cell. In this case, their separation is more challenging and particularly the detection of structural differences with polarization becomes rather limited. Nevertheless, in the following a short outlook limited to C-band is given concerning the observation of physical dynamics in the wheat (W) and the barley (B) field (indicated in Fig. 2) from the changes in the power ratios over the acquisition period.

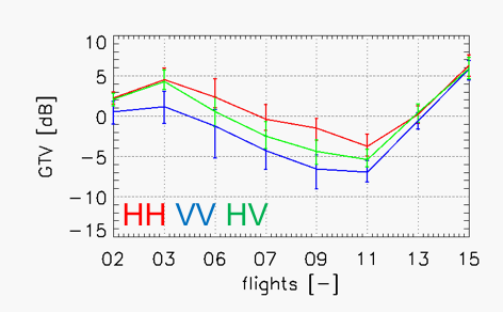

Figure 9: Variation of the ground-to-volume power ratio in W over the acquisition period.

The ground-to-volume power ratio for the W field shown in Fig. 9 is always higher in HH than in VV. Its decrease until flight 07 is related to the ongoing growth of the wheat. Starting from flight 09, the vegetation water content decreases from an average level of 90% in the earlier dates to 75% (flight 09), 60% (flight 11) and finally 20% (flight 13) before the plants are harvested in flight 15. The drying of the plants causes p_G to increase during the whole process. But initially (09-11) the drying process also effects a deeper penetration of the electromagnetic wave into the vegetation volume. Hence, scattering comes from a bigger part of the vegetation such that the dominating increase in p_V is the reason for a further decrease of the ground-to-volume ratio. Due to the more advanced drying process after flight 11, the vegetation becomes more transparent and p_V decreases leading to an increase in ground-to-volume ratio. The loss of water content in the vertical stalks at this stage makes the bended heads the dominant scattering particles in the volume. Therefore the decrease of p_V is stronger in VV than in HH reflected also in the only remarkable peak (ca. 3 dB) of the co-polar power ratio observed in flight 13.

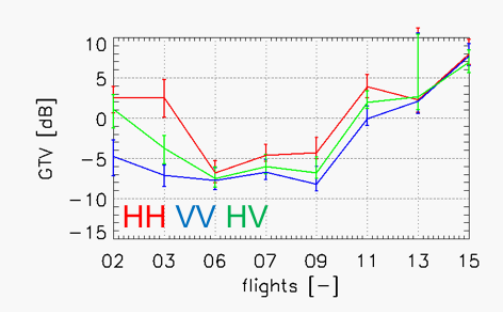

Figure 10: Variation of the ground-to-volume power ratio in B over the acquisition period.

Also in the barley the variation of the ground-to-volume power ratio (see Fig. 10) matches the physical changes observed from the ground measurements. For instance, in flight 03 the plants are vertically oriented and therefore much more volume and less ground scattering is present in VV compared to HH resulting in a difference between the ground-to-volume ratios of almost 10 dB. The bending of the (still milky) heads of the plants between flight 03 and 06 leads to a very strong increase of p_V in HH

assimilating the ground-to-volume ratios in the polarizations. Further, the drying process, starting from flight 09, can be detected by the increasing ground-to-volume ratio. Even though the Frobenius distance is very low throughout the whole study period for both species, the observations from the power ratios correlate with the variation of Δ. Hence, geometric differences in the plants are present and can be detected by the polarimetric variations of the powers. However, due to the low vegetation height in these fields, the vertical structure does not show significant differences between the polarizations.

4 Conclusions

After coherently separating the ground and volume scattering components, the polarimetric variation of the ground-to-volume ratio was analyzed in order to connect physical changes with the different scattering mechanisms ongoing in the acquisition dates. A measure evaluating structural differences between the polarizations was introduced to investigate the presence of orientation effects.

For instance, it has been seen, that at C-band, in the later development stages of the corn the main scattering contribution comes from the middle part of the plant where the fruit is actually developed. This does not imply any differential extintion effects since the structure changes in all polarizations in the same way. Also the size of the multi-look cell used for inversion has to be taken into account when evaluating the significance of orientation effects. When using a larger number of looks structures might become more random due to averaging. While at X-band the behaviour is similar than at C-band, at L-band a stronger sensitivity to the vertical stalks in the corn is evident in later dates.

For agricultural fields with low height compared to the vertical resolution, such as wheat and barley, the variation of the ground-to-volume ratio in the different polarizations over time allows to track physical changes in the vegetation, as for instance the bending of the heads or the drying of the plants. Even though such events are characterized by clear scattering power differences between the polarizations, the vertical resolution in these fields is too low for significant differences of the vertical structure function with polarization.

In future, it has to be investigated to which extent the acquisition scenario can be reduced to a lower number of trakcs still ensuring a reliable retrieval of the variations of the powers and the structural parameters.

5 Acknowledgements

We like to thank the team from the Department of Geography at the Ludwig-Maximilians University in Munich for their help in the ground parameter collection. This study was funded by the Helmholtz Alliance HA-310 "Remote Sensing and Earth System Dynamics", through the Initiative and Networking Fund of the Helmholtz Association, Germany.

References

[1] M. Pichierri, I. Hajnsek, and K.P. Papathanassiou, "A Multi-Baseline Pol-InSAR Inversion Scheme for Crop Parameter Estimation at Different Frequencies," *IEEE Transactions on Geoscience and Remote Sensing (submitted)*, 2015.

[2] J. D. Ballester-Berman, J. M. López-Sánchez, and J. Fortuny-Guasch, "Retrieval of Biophysical Parameters of Agricultural Crops using Polarimetric SAR Interferometry," *IEEE Transactions on Geoscience and Remote Sensing*, vol. 43, no. 4, pp. 683–694, 2005.

[3] H. Joerg, M. Pardini, and I. Hajnsek, "Spatial And Temporal Characterization of Agricultural Crop Volumes by means of Polarimetric SAR Tomography at C-band," in *Proceedings of International Geoscience and Remote Sensing Symposium (IGARSS), Milan*. IEEE, 2015.

[4] I. Hajnsek, R. Scheiber, L. Ulander, A. Gustavsson, G. Sandberg, S. Tebaldini, A. Monti Guarnieri, F. Rocca, F. Lombardini, and M. Pardini, "Technical Assistance for the Development of Airborne SAR and Geophysical Measurements during the BioSAR 2007 Experiment," *ESA, Paris, France, Tech. Rep*, vol. 22052, no. 08, 2009.

[5] C. Lopez-Martinez and A. Alonso-Gonzalez, "Assessment and Estimation of the RVoG Model in Polarimetric SAR Interferometry," *Geoscience and Remote Sensing, IEEE Transactions on*, vol. 52, no. 6, pp. 3091–3106, 2014.

[6] S. Tebaldini, "Algebraic Synthesis of Forest Scenarios from Multibaseline PolInSAR Data," *IEEE Transactions on Geoscience and Remote Sensing*, vol. 47, no. 12, pp. 4132–4142, 2009.

[7] M. Pardini and K.P. Papathanassiou, "Sub-Canopy Topography Estimation: Experiments with Multibaseline SAR Data at L-band," in *Geoscience and Remote Sensing Symposium (IGARSS), 2012 IEEE International*. IEEE, 2012, pp. 4954–4957.

[8] B. Ottersten, P. Stoica, and R. Roy, "Covariance Matching Estimation Techniques for Array Signal Processing Applications," *Digit. Signal Process.*, vol. 8, no. 3, pp. 185–210, 1998.

[9] K. Werner, M. Jansson, and P. Stoica, "On Estimation of Covariance Matrices with Kronecker Product Structure," *IEEE Transactions on Signal Processing*, vol. 56, no. 2, pp. 478–491, 2008.